

## A New Finger-Knuckle-Print ROI Extraction Method Based on Two-Stage Center Point Detection

Hongyang Yu, Gongping Yang, Zhuoyi Wang and Lin Zhang

School of Computer Science and Technology, Shandong University  
Jinan 250101, P.R. China  
Email: [gpyang@sdu.edu.cn](mailto:gpyang@sdu.edu.cn)

### Abstract

*Finger-knuckle-print (FKP) pattern has been utilized in biometric recognition systems. This paper proposes a new FKP region of interest (ROI) extraction method based on two-stage center point detection. In our method, a center point preliminary detection is constructed to capture the center point initially. Then, an efficient center point positioned algorithm is presented to locate the center point more precisely in real time. Finally, we select the Hong Kong Polytechnic University (PolyU) database to verify the efficiency of the proposed method. The experimental results show that the proposed method can extract ROI not only accurately but also in real time.*

**Keywords:** *biometric recognition, finger-knuckle-print, ROI extraction, two-stage center point detection*

### 1. Introduction

Biometric features have been widely used in personal authentication system. Compared with conventional recognition characteristics such as PIN number, biometric feature is more reliable and convenient. It can be used to distinguish individuals with their inherent physical and behavioral characteristics. In the past three decades, many biometric characteristics have been investigated, such as fingerprint, face, palm print, hand geometry, voice, gait, signature, *etc.* [1].

Among various kinds of biometric identifiers, recently, some scholars have reported that finger-knuckle-print pattern could act as a distinctive biometric identifier because of its highly inimitable pattern [2-4]. Unlike fingerprint, FKP is more unlikely to be abraded because people hold stuff with the inner side of the hand. And for the same reason, it is less possible to leave FKP on stuff. As a result, the private data leakage is more impossible. These advantages promote the research for FKP pattern in the future.

Many researches have shown that the identification performance of FKP is highly connected with the accuracy of the extraction of region of interest (ROI) [3, 6, 7], which contains abundant texture features [3]. In [3], Zhang, *et al.*, defined a window to extract ROI based on convex direction coding but its time complexity is too high, thus their method cannot meet the real-time requirement in some cases. In [8], Zhang, *et al.*, proposed an effective FKP recognition scheme by extracting and assembling local and global features of FKP images, which is based on the results of psychophysics and neurophysiology studies that both local and global information is crucial for the image perception. By increasing the scale of Gabor filters to infinite, they got the Fourier transform coefficients of the image, which was used as the global features. This scheme exploited both local and global information for FKP verification, where global information was also utilized to refine the alignment of FKP images in matching.

Although many methods perform effectively with normal images, they cannot keep high accuracy with skewed images. Based on the analysis of numerous FKP images, we find two kinds of skewed finger conditions, the skew in the horizontal direction and that

in the vertical direction, which are shown in Figure 1(a) and Figure 1(b), respectively.

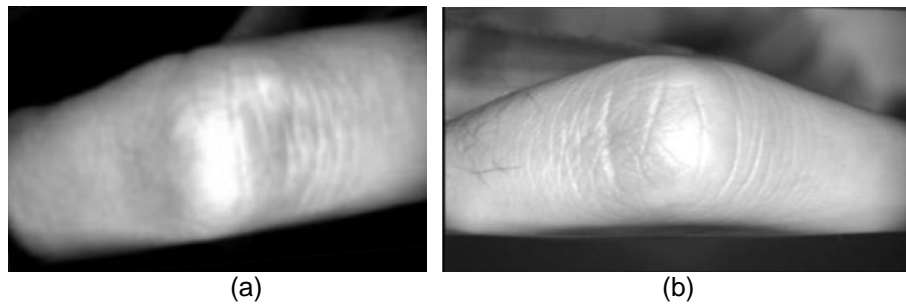


**Figure 1. Two Kinds of Skewed Finger Conditions: (a) Skew in the Horizontal Directions; (b) Skew in the Vertical Directions**

Thus, as for FKP recognition, the previous methods might be challenged by the decreasing in accuracy faced with the skewed finger conditions, especially when the skewed angle is large. One approach to solve these abnormal conditions is to introduce the concept of center point [5]. In [9], Kong, *et al.*, put forward a ROI extraction method based on center point detection and showed the effectiveness in experiments. However, they only considered the skew in the horizontal direction, while neglected the skew in the vertical direction, thus the method could not perform well.

To improve the positioning accuracy in skewed conditions, in this paper, we propose a new ROI extraction method based on two-stage center point detection. Four experiments are conducted on the open database from the Hong Kong Polytechnic University [10] to evaluate the performance of the proposed method. Experimental results demonstrate that the proposed method can perform well not only in recognition accuracy, but also in speed.

The rest of this paper is organized as follows. Section 2 introduces the proposed method including preprocessing, two-stage center point detection and ROI extraction. Section 3 describes the experiments in detail and discusses the experimental results. Section 4 presents the conclusion and future work.

## 2. The Proposed Method

In this section, we present a new ROI extraction method for FKP image, which is composed of three basic steps: firstly, the preprocessing is operated. Secondly, a two-stage center point detection method is proposed to detect the center point. At last, the ROI from FKP images is extracted based on the center point and the width of fingers. The ROI extraction process is illustrated in Figure 2.

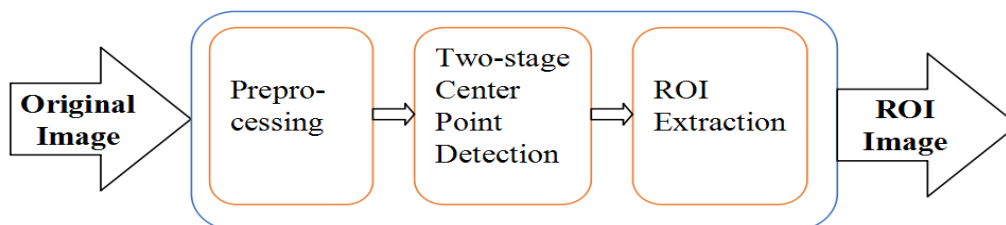


**Figure 2. The Proposed ROI Extraction Method**

### 2.1 Preprocessing

Because of some random noise and imperfect placement in image capture, it is necessary to remove the noise and correct the skewed image before ROI extraction. Image preprocessing can reduce the complexity of subsequent image processing. In this section, we will take the following preprocessing. Firstly, Gaussian filter is used to eliminate

random noise in original FKP images. Secondly, skewed images are detected and corrected in the horizontal direction.

**2.1.1. Eliminating Random Noise:** In the image acquisition process, original images might be influenced by various noises, which have negative influence on the quality of images. Thus, denoising is necessary.

Based on consideration above, we choose a suitable filter, which can denoise effectively and meanwhile respect the sharpness of the original images. In paper [3, 11], they proved that the Gaussian filter can not only effectively denoise the salt-and-pepper noise, but also preserve the edge details in image deblurring. In 2-D, an isotropic (*i.e.* circularly symmetric) Gaussian has the form in Equation (1) to remove the noise as a linear filter:

$$G(x, y) = \frac{1}{2\pi\sigma^2} e^{-\frac{x^2+y^2}{2\sigma^2}}, \quad (1)$$

where  $\sigma$  determines the width of the Gaussian and  $x, y$  refer to the coordinate. The following weight array will be obtained by Figure 3, we set  $\sigma = 1$ .

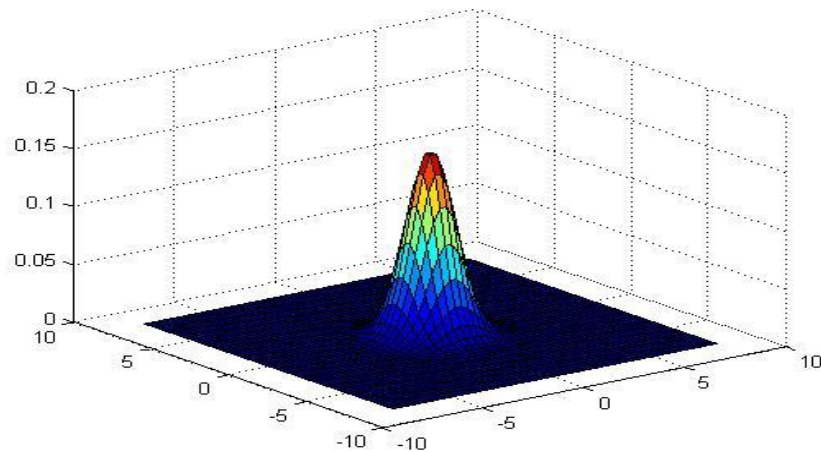


**Figure 3. 2-D Gaussian Distribution with Mean (0, 0) and  $\sigma=1$**

From Figure 3 we know that our experiment should choose a proper value for  $\sigma$  to obtain a convolution mask with size of  $a*b$ . From paper [12], we can compute the convolution result of original image  $f(x, y)$  and  $g(x, y)$ . The computation formula is in Equation (2):

$$h(x, y) = f(x, y) \cdot g(x, y) = \sum_{k=-a}^a \sum_{l=-b}^b f(x+k, y+l) \cdot g(k, l), \quad (2)$$

where parameter  $a$  and  $b$  determine the size of the convolution mask, and  $h(x, y)$  is the output image. In our paper,  $a$  and  $b$  will be obtained from Gaussian distribution in Figure 3, we set the value as  $a = b = 2$ . The significance of this convolution is that the output pixel values will be normalized when the convolution is performed. Consequently, it could ensure that intensity is not affected.

**2.1.2. Correcting Skewed Images in the Horizontal Direction:** As we stated above, plenty of FKP images show a certain degree of skew in the horizontal direction. In this section, we will address this issue to improve the robustness of the recognition system [13]. The correction process is expected to enhance the precision of center point of FKP and hence to improve the accuracy of ROI extraction.

Some researchers have detected the lower edge of the finger using Canny Edge Detection [14, 15]. According to the structure of the image acquisition device, fingers are put flatly when the FKP images are captured. Thus, the lower edge of finger in FKP image is stable and almost a straight line. In this paper, linear fitting method is used to fit a straight line under the lower edge. So we define the fitting equation as

$$y = ax + b, \quad (3)$$

where parameter  $a$  is the slope between finger and horizontal line, and  $b$  is y-intercept. In the Figure 4, we synthesize the line  $L_{oc}$ , which is detected by Canny Edge Detection. By the trigonometric function, we could get the value of angle  $\theta$  between the line  $L_{oc}$  and the horizon line  $L_{ox}$ , which should be computed by

$$\theta = \arctan a. \quad (4)$$

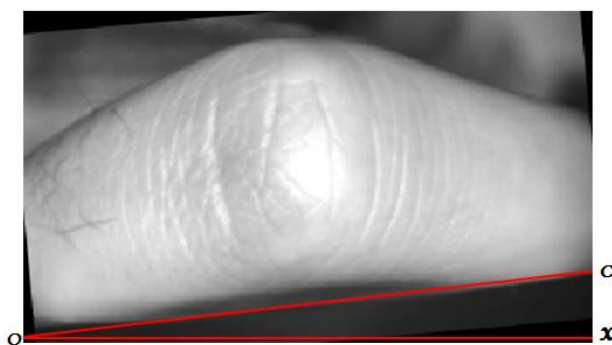


**Figure 4. The Skewed Image with the Obvious Tilt Angle**

Based on the detected sloped angle in Equation (4), we give the corrected solution of the skewed image. If the  $\theta > 0$ , the image will be rotated clockwise; if the  $\theta < 0$ , the image will be corrected counterclockwise. Otherwise, the image will not be rotated. Next, the correlation of the skewed image will be performed in the plane-coordinate system. In such system, point  $P_1(X_0, Y_0)$  is any pixel in original image, and point  $P_2(X_1, Y_1)$  is the point which corresponds to  $P_1$  after correction, The correction process in the coordinate system is shown in Figure 5, and the related variables are defined in Table 1.

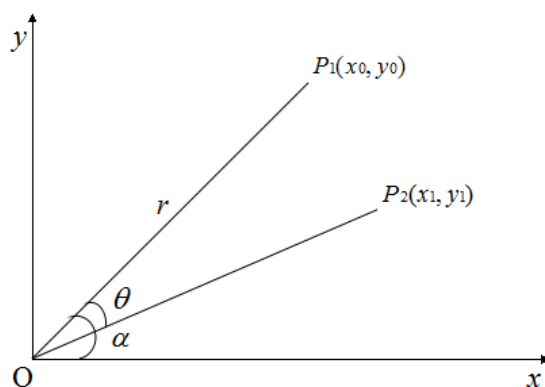


**Figure 5. The Correction Process in the Coordinate System**

**Table 1. Related Variables in the Coordinate System**

Variables	Description
$R$	The distance between origin point O and $P_1$
$\alpha$	The angle between $P_1$ and the X-axis
$\theta$	The detect slope angle

After the rotation of image, we could capture the coordinate value of the corresponding point P2 through trigonometric function as follows:

$$X_1 = r \cos(\alpha - \theta) = r \cos \alpha \cos \theta + r \sin \alpha \sin \theta \quad (5)$$

$$Y_1 = r \sin(\alpha - \theta) = r \sin \alpha \cos \theta - r \cos \alpha \sin \theta \quad (6)$$

In the actual operation, the values of  $X_1$  and  $Y_1$  might become decimals after the correction, while pixel coordinates are integers. So the correction process of the skewed image is an interpolation process for the coordinate values of the corrected image.

There are three optional interpolation methods: nearest-neighbor interpolation, bilinear interpolation and bicubic interpolation [16]. We choose bilinear interpolation because bilinear interpolation can reduce jaggies with a relatively low complexity, while the nearest-neighbor interpolation will produce too many jaggies, which will impact the effect of recognition, and bicubic interpolation's computation complexity is very high.

## 2.2 Two-stage Center Point Detection

After the preprocessing, we have eliminated random noise and corrected the skewed image in the horizontal direction. Then, we could detect the center point. From the FKP images, we could find that the brightest area is related to the center point. The ROI extraction method in [9] is based on the assertion that the center of the brightest area is the center point of FKP. However, this assertion is not accurate in some conditions, especially when the image skews in the vertical direction, which showed in Figure 6. Thus, we propose two-stage center point detection method, which could deal with the skewed images in the vertical direction. The method has two stages to detect the center point: in Stage I, we will detect the brightest area in FKP images and roughly regard the center of the area as the initial center point; in Stage II, we will relocate the center point according to the angle of the finger skewed in order to pinpoint the precise position. The detailed steps for extracting ROI are as follows.

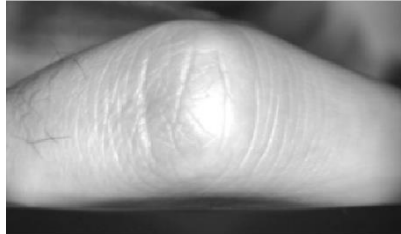


**Figure 6. The Image Skews in the Vertical Direction**

**2.2.1 STAGE I: Center Point Preliminary Detection:** Based on the previous description, the brightest area in FKP image has an connection with the center point. So in general condition, the center point of the brightest area could be regarded as the center point of FKP. We call the process Center Point Preliminary Detection.

In this stage, we define a window and calculate the average gray value of all pixels within the window. Then the window is moved from the center of the picture to four directions. In this paper, we move the window five pixels each time. If the average pixel value within the window becomes smaller, then stop making progress in this direction and change a direction moving again. The flow diagram is showed in Figure 7.

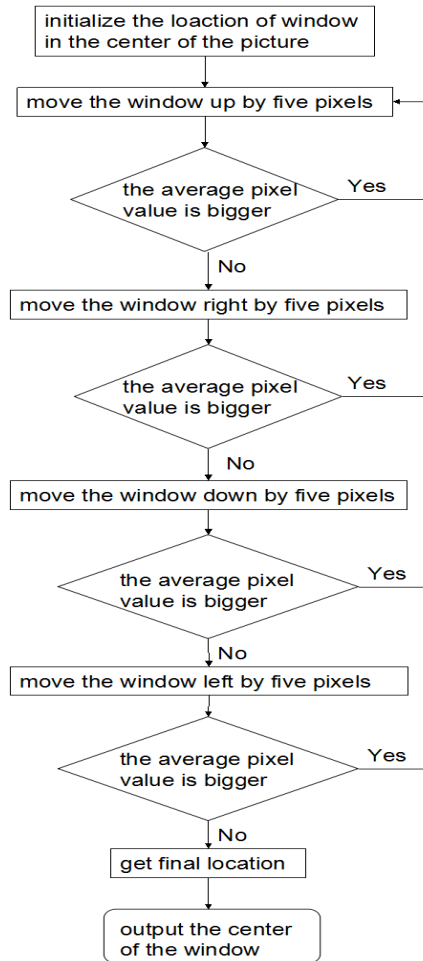


**Figure 7. The Flow Diagram of Center Point Preliminary Detection**

Because there is only one maximal value of the average pixel value, we can get the maximum average pixel value by this method. The average pixel value within the window can be calculated by Equation (7):

$$C(x, y) = \arg \max \left\{ \sum_{i=y-\frac{h}{2}}^{y+\frac{h}{2}} \sum_{j=x-\frac{w}{2}}^{x+\frac{w}{2}} \text{Picture}(i, j) \right\}, \quad (7)$$

where  $(x, y)$  is the coordinates of the center of window, and  $C(x, y)$  is the average pixel value within the window.  $w$  is the window's width, while  $h$  is the height.  $\text{Picture}(i, j)$  is the pixel value in point  $(i, j)$ . In the experiment we have tried different  $w$  and  $h$ , from various experiment results, it showed that  $w=30\text{px}$  and  $h=50\text{px}$  give the best effect.

The image processed by center point preliminary detection is shown in Figure 8.

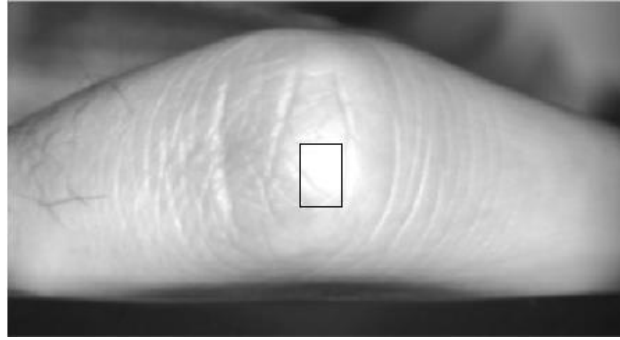


**Figure 8. The Image Processed by Center Point Preliminary Detection and the Frame Shows the Brightest Window Area**

**2.2.2 STAGE II: Center Point Secondary Precise Positioning:** From 2.2.1, we know that the center point of FKP will deviate from the brightest area when the images slant in the vertical direction. In order to detect the center point more precisely in this condition, we relocate the preliminary center point. Based on the characteristics of FKP images, we conclude that the more the angle of the finger skewed, the more the deviation between the initial center point detected in Stage I and actual center point of FKP. Thus, the key is to find the connection between the skewed angle and the position of the center point. We call the process Center Point Secondary Precise Positioning.

To simplify the model, we regard the cross section of finger knuckle as an ellipse. The schematic diagram is shown in Figure 9. In Figure 9,  $p_1, p_2$  is the center point of FKP, and  $h_1, h_2$  is the point with the highest pixel value, which is the point of intersection of the line  $L$  and ellipse. For the left ellipse, the highest pixel value is exactly the center point of finger knuckle print. For the right ellipse, the highest pixel value is below the center point.

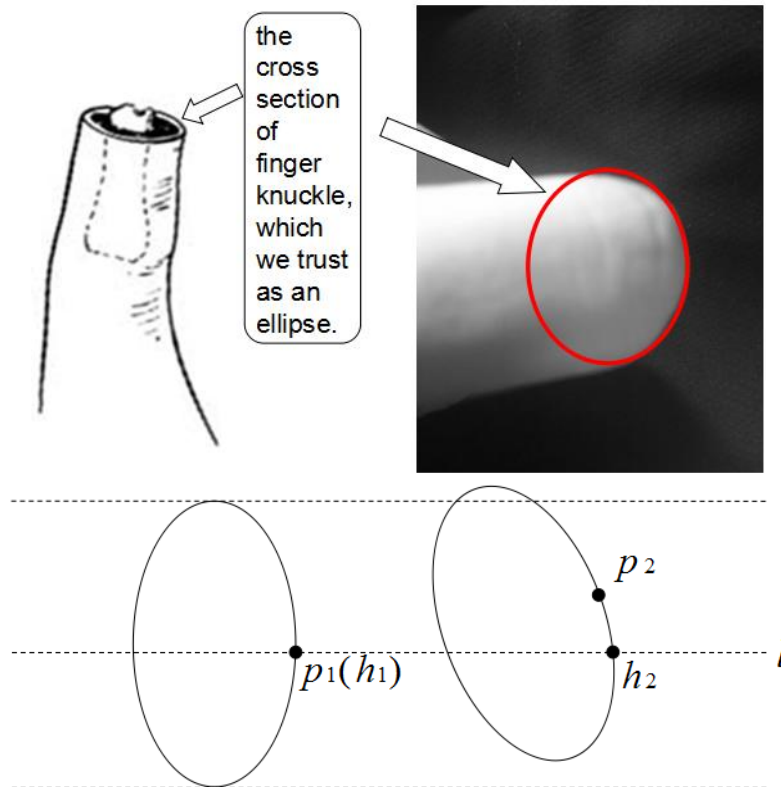


**Figure 9. The Cross Section of Finger Knuckle Image**

Based on this assumption, the function plots are shown in Figure 10. The formula of the ellipse is

$$\frac{y^2}{a^2} + \frac{x^2}{b^2} = 1, \quad (8)$$

where  $a$  is the width of the figure, and because the result is insensitive to  $b$ , in this paper, we set  $b = 0.8a$  based on the analysis of numerous images.

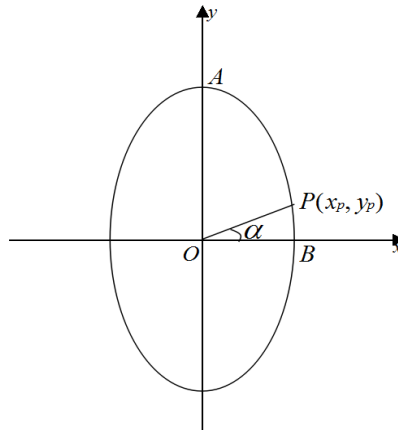


**Figure 10. Ellipse of the Cross Section of Finger Knuckle, the Angle between Line OP and X-axis Positive Direction is  $\alpha$**

The equation of line OP is

$$y = \tan \alpha \cdot x, \quad (9)$$

where the angle between line OP and X-axis positive direction is  $\alpha$ .

Then by simultaneous equations (8) and (9) we can calculate  $y_p$ , the y-coordinate of point  $P(x_p, y_p)$ :

$$y_p = \frac{ab \tan \alpha}{\sqrt{a^2 + b^2 \tan^2 \alpha}}. \quad (10)$$

Because the upper edge of the proximal phalanx finger is a straight line, we use Canny Edge Detection and Hough Transformation [14, 15] to detect the upper edge of the finger and then calculate the tilt angle. The line of the upper edge is shown in Figure 11. Then, we use the Equation (3) and Equation (4) in Section 2.1.1 to gain the angle  $\beta$  of upper edge. The angle  $\beta$  will be performed in the plane-coordinate system. In such system, we define Point A as the origin point, the corresponding point  $B(x_0, y_0)$  in Figure 12.

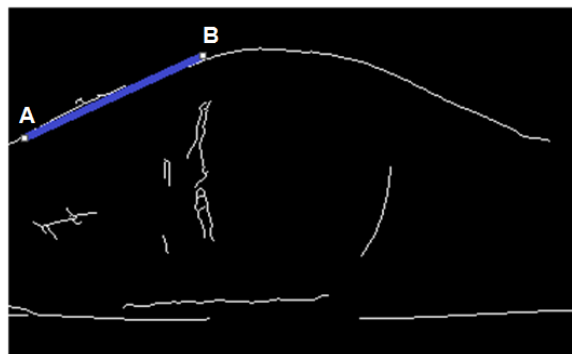


**Figure 11. The Image of the Line of Upper Edge**



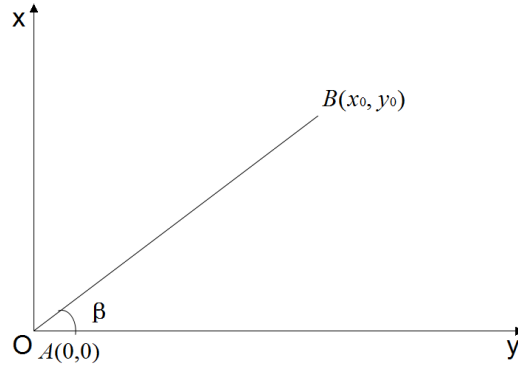


**Figure 12. The Angle  $\beta$  in the Plane-coordinate System**

$\theta$  and  $\beta$  is the projection angle in different direction. The angle  $\theta$  indicates the deviation of the center point, and the angle  $\beta$  indicates the skew of finger. So the relationship of the angle  $\theta$  and angle  $\beta$  is calculated by Equation (11).

$$\tan \theta = k \tan \beta. \quad (11)$$

According to analysis of the FKP images, we define  $k=5$ . Thus, the center point of FKP is computed by Equation (12)

$$(x_1, y_1) = (x_0, y_0 + y_p). \quad (12)$$

With the Equation (10), Equation (11) and Equation (12), we propose an algorithm to position the center point precisely, which is called center point secondary positioning algorithm. The algorithm is shown in Table 2.

**Table 2. Center Point Secondary Positioning Algorithm**

---

Input: $x_0, y_0$ (coordinates of the preliminary center point), <i>img</i> (processed image of FPK)
Output: $x_1, y_1$ (the center point of FPK)
Begin module
<i>img</i> = Canny( <i>img</i> , <i>side</i> ); //Canny edge detection, <i>side</i> means left hand or right hand
$\beta$ = Hough( <i>img</i> ); //Hough Transformation
$\tan \theta = k \tan \beta$ ;
$y_p = \frac{ab \tan \alpha}{\sqrt{a^2 + b^2 \tan^2 \alpha}}$ ;
$y_1 = y_0 + y_p$ ;
return $x_1, y_1$ ;
End module

---

### 2.3 ROI Extraction

After getting the center point, we extract ROI based on the symmetry of FKP. The range of  $x$  and  $y$  is defined as follow

$$x \in (x_1 - \frac{l}{2}, x_1 + \frac{l}{2}), \quad y \in (y_1 - \frac{h}{2}, y_1 + \frac{h}{2}), \quad (13)$$

where  $l$  is the length of ROI image, and  $h$  is the width of ROI image.

To determine the value of  $l$ , we assume that the length of finger is greater than that of FKP image. Thus, according to the analysis by [3, 9, 17], we choose the value of  $l$  is equal to 220.

In order to determine the value of  $h$ , the width of finger deserves to be considered because the width is usually different. For instance, the width of the little finger is much

smaller than the width of thumb. Thus, the value of  $h$  depends upon the width of finger. The relationship between  $k_0$  and  $w$  (the width of finger) is defined by Equation (14) and  $w$  is defined by Equation (15).

$$h = k_0 \cdot w \quad (0 < k_0 < 1), \quad (14)$$

$$w = w_1 - w_2, \quad (15)$$

where  $w_1$  is the upper endpoint of upper line, which has been detected in Sect. 2.2.2.  $w_2$  is the lower endpoint of lower line, which has been detected in Section 2.1.1. According to experiments based on a large number of images, we determine the  $k_0 = 0.4$ . Some extracted ROI images are shown in Figure 13.

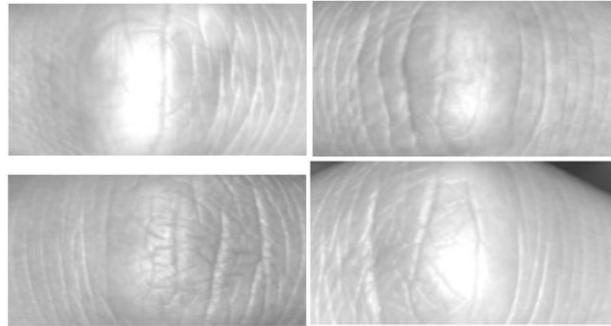


**Figure 13. The Extracted ROI Images by Using the Proposed Method**

### 3. Experimental Results

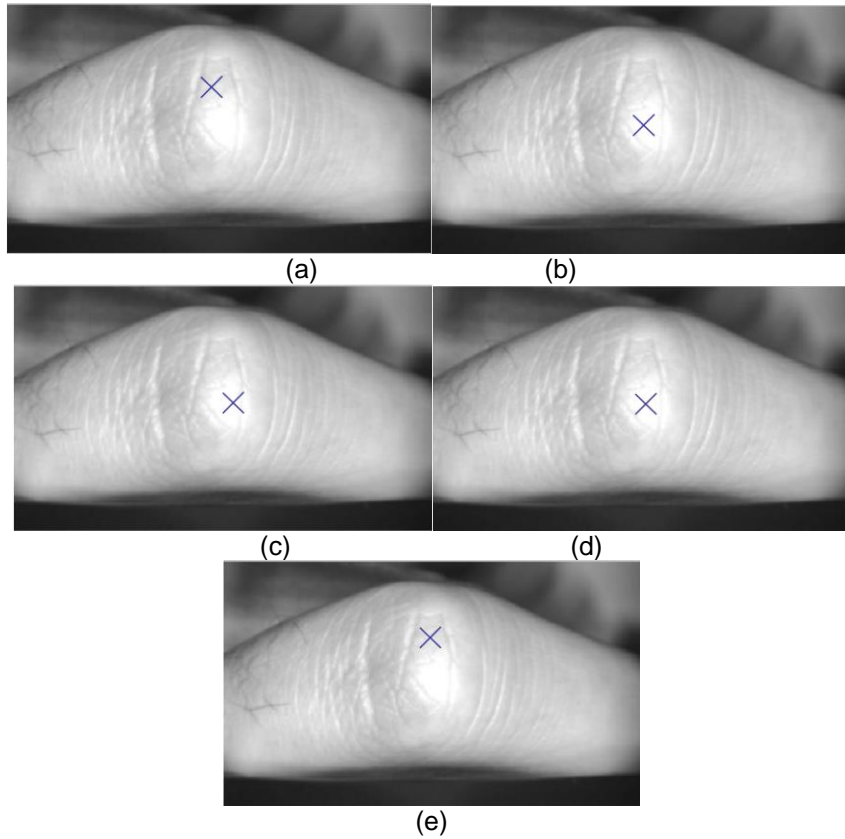
#### 3.1 Experimental Database and Settings

The proposed method is tested on the FKP database from the Hong Kong Polytechnic University [10] to evaluate the performance. The open database was gathered from 165 volunteers, including 125 males and 40 females, and contains 7,920 images from 660 different fingers. Among the volunteers, 143 subjects are 20 ~ 30 years old and others are 30 ~ 50 years old. Images of each user are collected in two separate sessions. For each user, index and middle finger of each hand have been acquired in each session. Images collected in first session are considered for training while the remaining ones are used for testing. The original image size is  $384 \times 288$ . The experiments are implemented in Matlab2010b on a PC with a 3.10 GHz CPU and 4.0 GB memory.

To show the performance of the proposed method comprehensively, four experiments are designed to evaluate the proposed method: In Experiment 1, the proposed method is compared with three other methods in terms of the accuracy of center point location of FKP. In Experiment 2, we compare the proposed method with three other methods in the aspect of the results of ROI extraction. In Experiment 3, the recognition performance of four methods is evaluated by the equal error rate (EER) and the receiver operating characteristics (ROC). Finally, the average processing times of four methods are measured in Experiment 4.

#### 3.2 Experiment 1

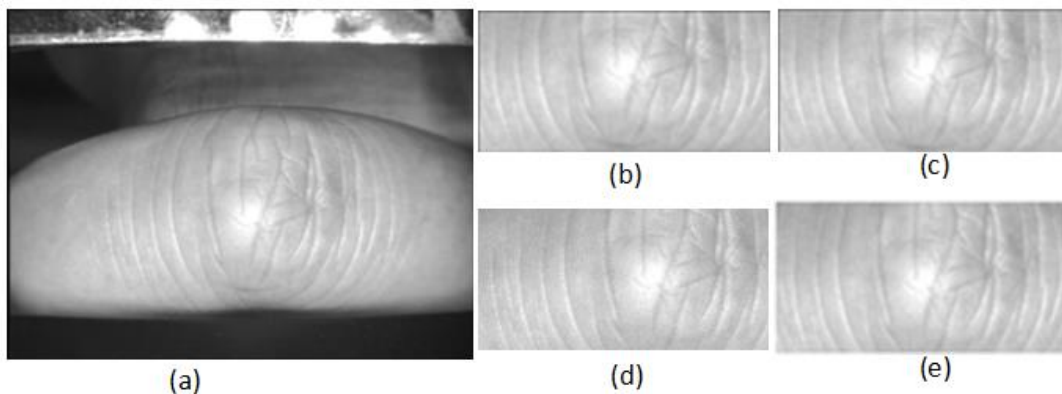
The most significant advantage of our method is the accuracy of center point detection. In this experiment, we will apply the two-stage center point detection method, which we proposed in 2.2, to locate the center point. The result shows in Figure14. We compare the result of different methods with artificial marked images. We could conclude that our method could perform more accurate in center point detection than Zhang's method [3], Ehteshami's method [17] and Kong's method [9].



**Figure 14. The Comparison of Center Point Detection: (a) Center Point is Manually Labeled; (b) Center Point is labeled by Zhang's Method; (c) Center Point is labeled by Ehteshami's Method; (d) Center Point is labeled by Kong's Method; (e) Proposed Method**

### 3.3 Experiment 2

In this experiment, we compare the ROI images extracted by our proposed method to the images extracted by three different extraction methods [3, 9, 17]. In order to be applied to some extreme conditions, the original FKP images are artificially randomly rotated at an angle from  $-30^\circ$  to  $30^\circ$ . In the following result, the original FKP images are shown in Figure 15a. The corresponding ROI images extracted by different methods are illustrated in Figure 15b-e respectively. The result visually reflects that our method is robust to different conditions. We could see that although various methods could perform well when the image is standard, the proposed method has better performance compared with other methods for skewed images.



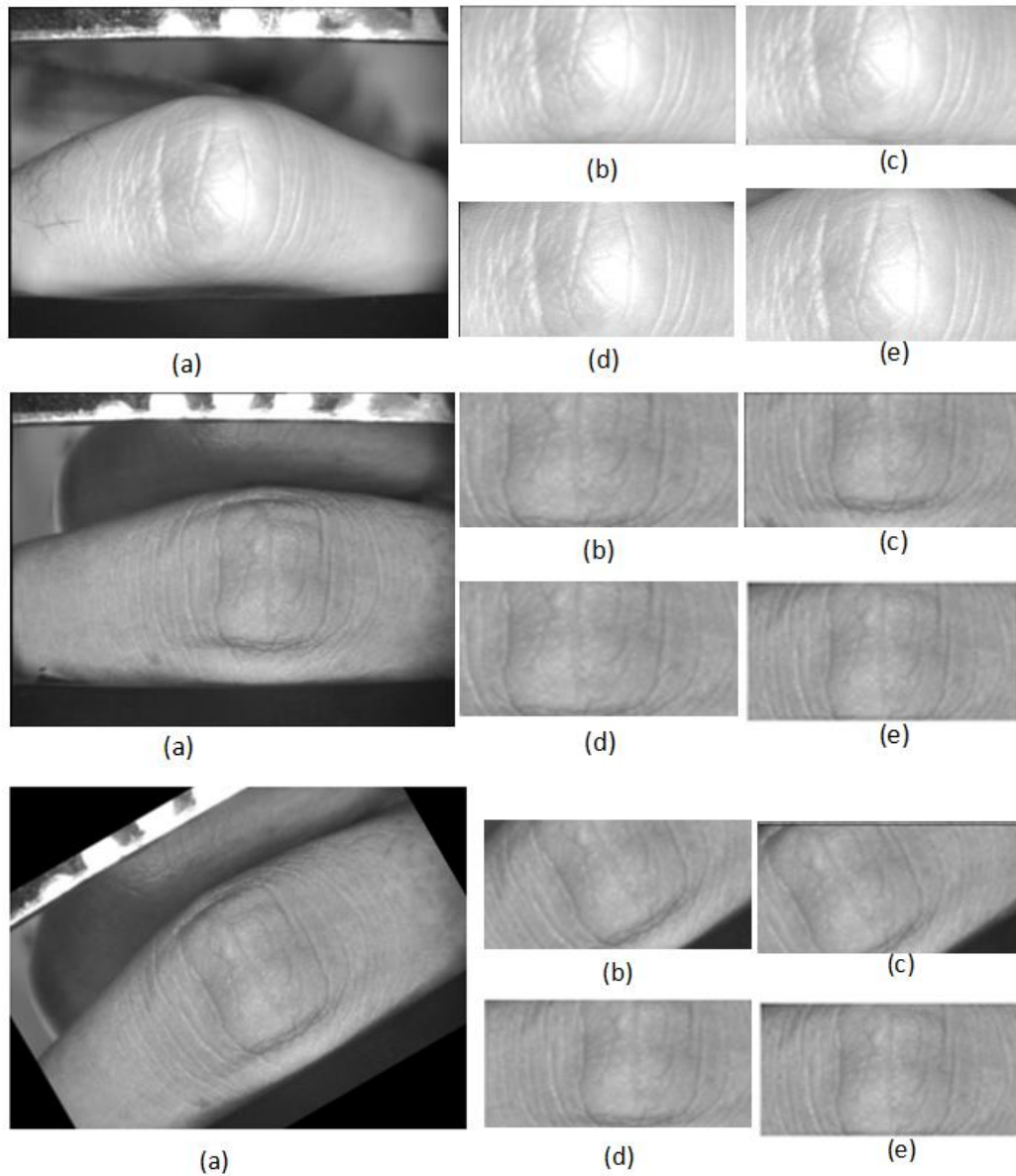


**Figure 15. The Extract Result of Method: (a) Original Image; (b) ROI is Extracted by Zhang's Method; (c) ROI is Extracted by Ehteshami's Method; (d) ROI is Extracted by Kong's Method; (e) ROI is Extracted by Proposed Method**

### 3.4 Experiment 3

In this experiment, the proposed method is compared with three existing ROI extraction methods [3, 9, 17] in terms of recognition rate in the verification mode. We use four types of FKP images from the open database, which respectively are the left index fingers, the left middle fingers, the right index fingers and the right middle fingers [10]. In this dataset, every type of finger has 165 classes and for each of the class, there are 12 images.

First of all, we divide each class into two categories, and each class contains 6 FKP images. The images in the first category are regarded as the sample set and the images in the second category are regarded as the test set. Secondly, we match each image in the test set with all images in the sample set. At last, this paper utilizes nearest-neighbor-ratio method [18] to compute the matching rate between different feature vectors. If two

matching images come from the different class, we define this match as the false reception; if two images from the same class cannot be matched, we define this phenomenon as the false rejection. In order to evaluate the performance of our method, we apply the EER as benchmark in biometric systems. And in terms of feature matching technique, we choose the Speeded-Up Robust Features (SURF) [19] method.

The experimental results of different methods are summarized in Figure 16, which describe the corresponding ROC.

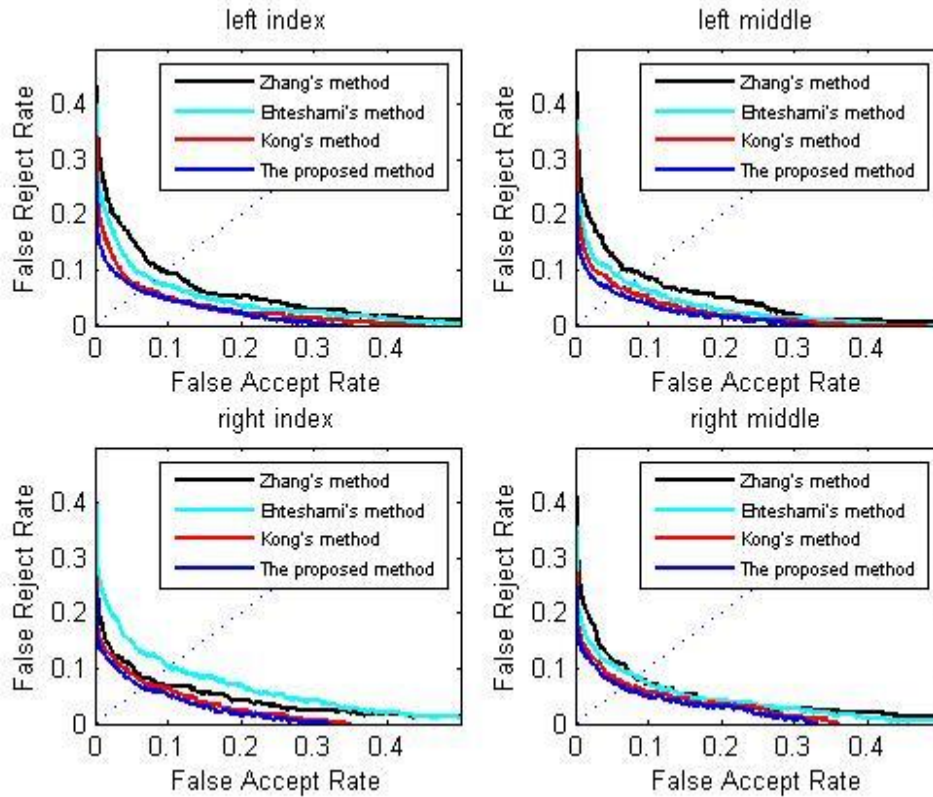


**Figure 16. ROC Curves by Different ROI Extraction Methods**

We can conclude from Figure 16 that our method achieves better performance than the three other methods. Zhang’s method cannot be effective when the texture features are not distinctness and the FKP are skewed. Ehteshami’s method cannot perform effectively when meeting skewed images compared with our method. Kong’s method cannot perform as well as our method in the vertical skewed direction, though the method can appear effectively in the horizontal skewed direction. Therefore, our method has a better prospect in processing the skewed image.

### 3.5 Experiment 4

In this experiment, the average running time of our proposed method is computed and compared with the time of three existing ROI extraction methods [3, 9, 17]. The time of the four ROI extraction methods are shown in Table 3.

**Table 3. The Processing Times of the Different ROI Extraction Methods**

Methods	Zhang’s method	Ehteshami’s method	Kong’s method	Proposed method
Time(ms)	208	160	103	125

From Table 3, we could obtain that average running time of the proposed method is 105 ms, which is faster than [3] and [17] but a little slower than Kong's method [9]. In conclusion, the proposed method is efficient enough to be applied in a real-time system.

#### 4. Conclusion and Future Work

In order to improve the accuracy of ROI extraction in various skewed conditions, we have proposed the ROI extraction method based on two-stage center point detection in this paper. We can correct the skewed images in both horizontal and vertical direction by more accurately detecting center point of FKP. The experiments, which are performed on open FKP database, show that the proposed method can extract ROI not only accurately but also in real time. Admittedly, there are also several disadvantages in our method. For example, some coefficients cannot change automatically according to brightness, and thus, when the brightness is too high or too low, the accuracy will be influenced. So our future work will be focused on changing coefficients automatically to further enhance the accuracy.

#### Acknowledgments

The work is supported by National Science Foundation of China under Grant No. 61472226 and Shandong Natural Science Funds for Distinguished Young Scholar under Grant No. JQ201316. The authors would like to thank the anonymous reviewers for their helpful suggestions.

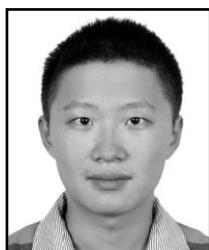
#### References

- [1]. Z. Stan and Li (Ed.), *Encyclopedia of Biometrics*, Springer, (2009).
- [2]. A. Morales, C. Travieso, M. Ferrer and J. Alonso, "Improved finger-knuckle-print authentication based on orientation enhancement", *Electronics Letters*, vol. 47, no. 6, (2011), pp. 380-381.
- [3]. L. Zhang, L. Zhang, D. Zhang and H. Zhu, "Finger-knuckle-print verification for personal authentication", *Pattern Recognition*, vol. 43, no. 7, (2010), pp. 2560-2571.
- [4]. L. Zhang, L. Zhang and D. Zhang, "Finger-knuckle-print: a new biometric identifier", In: *Proceedings of the IEEE International Conference on Image Processing*, (2009), pp. 1981-1984.
- [5]. K. Y. Cheng, and A. Kumar, "Contactless finger knuckle identification using smartphones", *BIOSIG-Proceedings of the International Conference of the Biometrics Special Interest Group*, (2012), pp. 1-6.
- [6]. A. Meraoumia, S. Chitroub and A. Bouridane, "Palmprint and finger-knuckle-print for efficient person recognition based on Log-Gabor filter response", *Analog Integr Circ Signal Process*, vol. 69, no. 1, (2011), pp. 17-27.
- [7]. M. Xiong, W. Yang and C. Sun, "Finger-knuckle-print recognition using LGBP", In: *Advances in Neural Networks-ISNN 2011*, Springer, Berlin, Heidelberg, (2011), pp. 270-277.
- [8]. L. Zhang, L. Zhang, D. Zhang and H. Zhu, "Ensemble of local and global information for finger-knuckle-print recognition", *Pattern Recognition*, vol. 44, no. 9, (2011), pp. 1990-1998.
- [9]. Kong, Tao, G. Yang, and L. Yang, "A new finger-knuckle-print ROI extraction method based on probabilistic region growing algorithm", *International Journal of Machine Learning and Cybernetics*, (2013), pp. 1-10.
- [10]. PolyU FKP Database, [http://www4.comp.polyu.edu.hk/\\*biometrics/FKP.html](http://www4.comp.polyu.edu.hk/*biometrics/FKP.html)
- [11]. Bar, Leah, N. Sochen, and N. Kiryati, "Image deblurring in the presence of salt-and-pepper noise", *Scale Space and PDE Methods in Computer Vision*. Springer Berlin Heidelberg, (2005), pp. 107-118.
- [12]. R. Jain, R. Kasturi and B. G. Schunck, "Machine vision", McGraw-Hill, USA, (1995).
- [13]. A. Arampatzis, G. D. Monte and K. Karamanidis, "Effect of joint rotation correction when measuring elongation of the gastrocnemius medialis tendon and aponeurosis", *J Electromyogr Kinesiol*, vol. 18, no. 3, (2008), pp. 503-508.
- [14]. P. Bao, L. Zhang and X. Wu, "Canny edge detection enhancement by scale multiplication", *IEEE Trans Pattern Anal Mach Intell*, vol. 27, no. 9, (2005), pp. 1485-1490.
- [15]. H. Liu and K. C. Jezek, "Automated extraction of coastline from satellite imagery by integrating Canny edge detection and locally adaptive thresholding methods", *International Journal of Remote Sensing*, vol. 25, no. 5, (2004), pp. 937-958
- [16]. S. Battiato, G. Gallo and F. Stanco, "Smart interpolation by anisotropic diffusion", In: *Proceedings of 12th International Conference on Image Analysis and Processing*, (2003), pp. 572-577.
- [17]. N. S. M. Ehteshami, M. Tabandeh and E. Fatemizadeh, "A new ROI extraction method for FKP images using global intensity", In: *2012 6th International Symposium on Telecommunications*, (2012), pp

1147–1150.

- [18].H. Bay, A. Ess, T. Tuytelaars and L. V. Gool, “Speeded-up robust features (SURF)”, *Comput Vis Image Underst*, vol. 110, no. 3, (2008), pp. 346–359.
- [19].G. S. Badrinath, A. Nigam and P. Gupta, “An efficient finger-knuckle-print based recognition system fusing sift and surf matching scores”, In: *Proceedings of the 13th International Conference on Information and Communications Security*, (2011), pp 374–387.

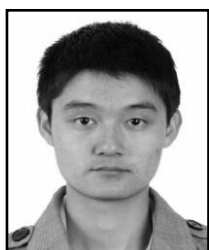
## Authors



**Hongyang Yu** he is studying for a Bachelor’s degree in School of Computer Science and Technology of Shandong University from 2011, his research interests are machine learning, data mining, biometrics, *etc.*



**Gongping Yang** he received his Ph.D. degree in computer software and theory from Shandong University, China in 2007. Now he is a professor in the School of Computer Science and Technology, Shandong University. His research interests are biometrics, medical image processing, and so forth.



**Zhuoyi Wang** he received his Bachelor degree in School of Computer Science and Technology of Shandong University in 2014, his research interests are data mining, pattern recognition, *etc.*



**Lin Zhang** He is studying for a Bachelor’s degree in School of Computer Science and Technology of Shandong University from 2011, his research interests are machine learning, data mining, pattern recognition, *etc.*

